



Waste Glass Reuse in Foamed Alkali-Activated Binders Production: Technical and Environmental Assessment

Shaoqin Ruan^{1,2}, Gediminas Kastiukas^{2*}, Shuang Liang² and Xiangming Zhou^{2*}

¹College of Civil Engineering and Architecture, Zhejiang University, Hangzhou, China, ²Department of Civil and Environmental Engineering, Brunel University London, Uxbridge, United Kingdom

OPEN ACCESS

Edited by:

Shengwen Tang,
Wuhan University, China

Reviewed by:

Joana Almeida,
Universidade NOVA de Lisboa,
Portugal
Xiaohong Zhu,
University of Leeds, United Kingdom
Fang Xu,
China University of Geosciences,
China

*Correspondence:

Gediminas Kastiukas
Gediminas.Kastiukas@brunel.ac.uk
Xiangming Zhou
Xiangming.Zhou@brunel.ac.uk

Specialty section:

This article was submitted to
Structural Materials,
a section of the journal
Frontiers in Materials

Received: 08 July 2020

Accepted: 27 August 2020

Published: 28 September 2020

Citation:

Ruan S, Kastiukas G, Liang S and Zhou X (2020) Waste Glass Reuse in Foamed Alkali-Activated Binders Production: Technical and Environmental Assessment. *Front. Mater.* 7:581358. doi: 10.3389/fmats.2020.581358

Waste glass is a type of construction and demolition waste, which carries significant environmental burdens and can be recycled. In this study, a foamed alkali-activated glass (FAAG) via the use of milled waste glass was synthesized in low-temperature (i.e., 80°C). The influence of foaming agent (i.e., aluminum powder) content on the foaming process of samples was investigated and optimized in view of their performance. The optimum mix formulation, which is FAAG with 10% aluminum powder was then selected, and followed by the measurement of the water-resistance and absorption, impact resistance and thermal conductivity of the prepared FAAG. X-ray diffraction was also involved to identify the phase formation within the samples. Finally, the environmental impacts related to the preparation of 1 kg FAAG were obtained. Results shows that a type of more sustainable FAAG compared with the commercial product was successfully developed in low-temperature, revealing the low thermal conductivity of ~0.13 W/(mK) with a density of ~0.59 g/cm³ and compressive strength of ~5.52 MPa, which is 97% higher than the commercial product. Meanwhile, in addition to a foaming agent, aluminum powder is also acting as a key component in the geopolymerization of samples, facilitating the formation of aluminosilicate that provides strength.

Keywords: construction and demolish waste, foamed alkali-activated glass, mechanical performance, thermal conductivity, environmental impacts

INTRODUCTION

In the European Union, construction and demolition waste (CDW) is becoming a serious issue, accounting for around 25–30% of all waste generated. CDW can be categorized into several groups such as concrete, bricks, wood or glass. Among them, in 2018, 27 metric million tons of glass is produced and only 21% of them are recycled (Statista, 2018). At present, CDW including waste glass was mainly disposed and treated via the procedures of landfilling or incineration, and (Zaman, 2010) reported that landfilling presented significantly lower environmental burdens than incineration due to fewer emissions produced and no direct heat required. In order to increase add-value of CDW and potentiate the circular economy, the reuse of secondary resources is highly recommended by European Commission targets (European Commission, 2020). For instance, 67% of waste glass was recycled in United Kingdom (Lebullenger and Mear, 2019). However, it is also indicated that owing to a large land requirement and difficulty in monitoring emissions in a long time, there are more

restrictions in terms of landfilling of waste in the developed countries (Zaman, 2010). Therefore, the reuse of waste glass in the area of construction provides an alternative solution to its disposal. Currently, a simple option of waste glass under exploration is in the replacement of virgin aggregates in concrete (Lu et al., 2019; Xiao et al., 2020). Besides, the use of waste glass treatment in the construction sector is also investigated. For instance, it can be used in the preparation of alkali-activated binders or geopolymers.

Alkali-activated binders or geopolymers have been widely studied due to their potential applications which can be environmental friendly (Ma et al., 2018) and can replace Portland cement (PC) in several niche applications (Panda et al., 2019; Panda et al., 2020), and waste glass has also been utilized for their preparation. For instance, waste glass is capable of acting as an alkaline activator, which was proved to be effective for the hydration of the precursors (Torres-Carrasco and Puertas, 2015; Tchakouté et al., 2016). At the same time, waste glass can also be regarded as a precursor, however, its reactive alumina content is relatively low [i.e., 0–5% (Metro)], which inhibits its geopolymerization. Therefore, some additives containing alumina should be added such as calcium aluminum cement, which resulted in the formation of sodium-aluminosilicate (N-A-S-H) gel as well as a densified microstructure, contributing to the improvement of the compressive strength of samples (Luhar et al., 2019). At the same time, (Vafaei and Allahverdi, 2017), also synthesized geopolymers *via* the usage of waste glass and calcium aluminate cement, and a more cross-linked network was formed within the samples with higher compressive strength revealed. In addition to calcium aluminum cement, waste glass is also widely mixed with metakaolin to produce geopolymers. For instance, Si et al. (2020) demonstrated that the incorporation of waste glass into the metakaolin-based geopolymer samples led to the formation of a denser gel structure with a refinement of pore structure. Besides, the shrinkage of geopolymers, which is a serious issue in hardened samples (Yang et al., 2017; Zhu et al., 2018), also reduced due to the refinement of their pore structure so that a reduction in the moisture loss rate was achieved within the samples (Si et al., 2020). Also, Bai et al. (2019) developed waste glass-based cellular geopolymers with the use of a stabilizing agent, which revealed thermal conductivity of ~ 0.21 W/mK and compression strength of ~ 7.3 MPa.

In the meantime, some precursors such as tungsten mining waste are also short of a silica source during the geopolymerization, therefore, Kastiukas and Zhou (2017) reported that the incorporation of waste glass into alkali-activated tungsten mining waste was capable of providing an additional silica source, leading to the formation of (C, N)-A-S-H phases within the samples as well as a boost of their mechanical strength. Further, accompanied by an increment of strength, it was also revealed that the addition of glass cullet and powder into alkali-activated binders resulted in an improvement of their workability and fire-resistance (Lu and Poon, 2018) with low thermal conductivity presented (Xuan et al., 2019).

Foamed geopolymers or alkali-activated binders, which is a recent innovation, present the benefits of foamed concrete and

geopolymers, and they are capable of reducing the environmental impacts of construction materials and offering new alternative materials for thermal insulation (Gu et al., 2020). Due to the excellent thermal insulation, foamed geopolymers can be prepared through a physical or a chemical foaming process. The physical foaming route consists of a mixture of geopolymers and precast foam prepared by a foaming agent, which would then produce a large number of pores inside the paste after setting, whereas the chemical one mainly mixes chemical foaming agent such as H_2O_2 and aluminum powders, followed by the production of H_2 and O_2 that introduced pores within the paste, as shown in Eqs. 1 and 2.



Unlike foamed geopolymer, there are also numerous studies investigating the performance of foamed glass as it has already been used as a thermal insulation material for the buildings, however, its preparation is an energy-intensive process where high temperature (i.e., 700–800°C) is required and emits CO_2 , which contributes to the global climate change. During the preparation of foamed glass, the raw glass is first ground and mixed with the carbon and Mn_3O_4 (i.e., foaming agent), and the mixture is then heated in high temperature with some protective atmosphere introduced such as non-oxidizing gases (e.g., Ar or N_2). During the heating process, CO_2 is produced to generate some pores within the glass, as shown in Eq. 3. Finally, it is necessary to cool down the newly produced foamed glass (König et al., 2019; Østergaard et al., 2019). Therefore, a foamed geopolymer based on the use of glass may be a better option than a foamed glass in terms the economic and environmental concerns.



As aforementioned, although waste glass is already used as a type of alkali-activator, or a partial replacement of slag, fly ash, etc, only a few studies investigated the use of 100% waste glass into the synthesis of alkali-activated binders especially foamed products. Besides, the produced foamed alkali-activated glass (FAAG) is different compared with the production process of foamed glass in terms of the production process, which avoids high temperature and CO_2 emission. Further, a comprehensive life cycle assessment in terms of the preparation is scarce in the literature, particularly considering the environmental impacts of waste glass treatment during the assessment.

Therefore, in view of the foregoing, this study fabricated a foamed alkali-activated binder based on 100% of waste glass, and the parameter that was investigated in this study was the content of the foaming agent (i.e., aluminum powder). The FAAG with 10, 20 and 30% aluminum powder were tested in this study. Consequently, the optimal content of foaming agent was selected and the corresponding samples were then prepared based on their mechanical performance and density. After that, the key performance of samples such as thermal conductivity, water, and impact resistance were explored and the outcomes were compared with the existing foamed products in the literature. Further, this study also performed a comprehensive life cycle

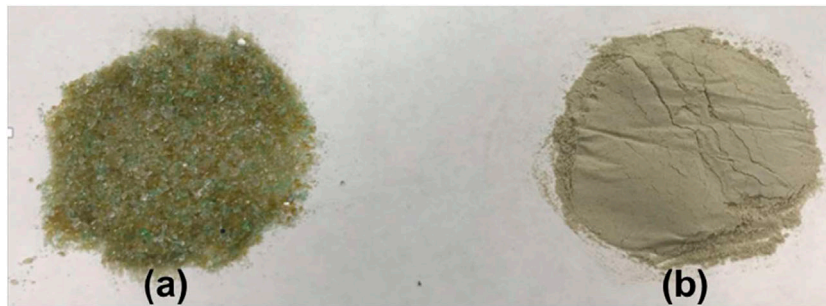


FIGURE 1 | Waste glass as received (A) and after milling (B).

assessment of FAAG preparation, where the environmental burdens related to the landfilling or incineration of waste glass were also taken into account, and the outcomes were then compared with a commercial aerated product.

MIX DESIGN, MATERIALS, AND METHODS

Raw Materials and Mix Design

The raw materials used to produce the FAAG in this study consisted of waste glass (received from the local municipality of Covilhã, Portugal), sodium hydroxide (NaOH, 98%) (Fisher Scientific, Germany), sodium silicate (Na_2SiO_3) (Solvay SA, Portugal), and aluminum powder (Sigma Aldrich, United Kingdom). The 10 M sodium hydroxide solution, prepared by dissolving sodium hydroxide pellets in de-ionized water, was combined with the sodium silicate solution consisting of a $\text{SiO}_2/\text{Na}_2\text{O}$ ratio of 3.23 (8.60 wt% Na_2O , 27.79 wt% SiO_2 , 63.19wt% H_2O , and 0.4wt% Al_2O_3), to form the alkali activator. The wavelength dispersive X-ray fluorescence was used to obtain the chemical composition of the waste glass (Na_2O :12.4%; MgO :1.8%; Al_2O_3 :2.1%; SiO_2 : 68.7%; SO_3 : 0.3%; K_2O : 0.8%; Fe_2O_3 : 1.5%; CaO : 10.0%). **Figure 1** shows the waste glass as received and after milling, respectively.

The waste glass was milled at 500 rpm for 20 min using a planetary ball milling machine (Retsch, PM 100, Germany) to achieve a powder consistency. The particle size distribution curve is illustrated in **Figure 2**. The activator solution was added to the precursor (i.e., waste glass) and blended using a bench-top mixer at 300 rpm for 5 min, forming the paste. Immediately after, the aluminum powder was added to the paste and followed by a further 30 sec of mixing. The paste was cast into polystyrene molds with the dimensions of 40 mm × 40 mm × 160 mm allowing for the foaming reaction between aluminum powder, water, and NaOH to take place, as expressed in **Eq. 1** already.

The freshly foamed samples were sealed and placed in a temperature and humidity controlled environmental chamber at 80°C and 75% relative humidity for 24 h, followed by 20°C and 75% relative humidity until the specific age (i.e., 7, 14, and 28 days) of testing. The $\text{Na}_2\text{SiO}_3/\text{NaOH}$, waste glass-to-activator and water-to-waste glass ratios were fixed at 3, 4.5, and 0.12 separately. Three levels of aluminum powder (i.e., 10, 20, and 30%) were investigated, and its optimal content was selected based on the mechanical performance and density. The mix design of FAAG samples in this study is shown in **Table 1**. The samples were then prepared, and the measurements of their water-resistance and absorption, impact resistance, thermal conductivity, and environmental impacts were performed later.

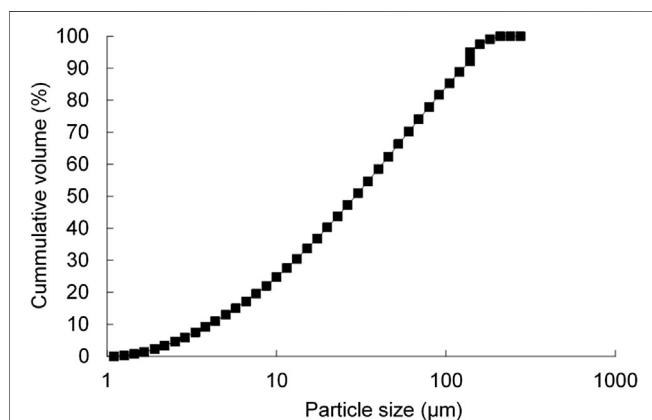


FIGURE 2 | Particle size distribution of milled waste glass powder.

Experimental Work

In the experimental work, the mechanical properties, density, water resistance, water absorption, impact resistance, and thermal conductivity of samples were tested. The use of X-ray diffraction (XRD) facilitates the understanding of phases within the samples. The details are shown as follows.

Mechanical Properties

The compressive and three-point bending of each sample were tested after 7, 14, and 28 days as specified by EN196-1 (2016) using a 25 kN universal testing machine (Instron 5960, United Kingdom) at a constant loading rate of 3 kN/min. The dimensions of samples are 40 mm × 40 mm × 160 mm during the mechanical strength test. The compressive and three-point bending values were the average ones obtained from three samples.

TABLE 1 | The mix design of foamed alkali-activated glass samples.

Precursor/activator ratio	Water/precursor ratio	Aluminium powders/NaOH mass ratio (%)	Na ₂ SiO ₃ /NaOH mass ratio
4.5	0.12	10	3
4.5	0.12	20	3
4.5	0.12	30	3

Density

The true density of the FAAG in triplicates was determined with a helium pycnometer (AccuPyc 1,340, Micromeritics, United Kingdom) in line with ASTM (2017). The device adopted some approaches of gas displacement and the relationship between the volume and the pressure relationship is known as Boyle's Law. The pycnometer is identified as a type of density measuring device, however, they are merely measuring volume actually, and density is obtained *via* a ratio of mass to volume; and the mass is also measured through the device by weighing.

Water Resistance

Six samples at the curing age of 14 days were dried for 24 h at a constant temperature of 80°C, weighed and then placed in a dry chamber for cooling without moisture absorption. The prisms were subsequently placed inside a container filled with de-ionized water and left at 20°C and 75% relative humidity to cure for a further 7 or 14 days. The mechanical performances of samples were determined, along with the strength retention coefficient as defined by Eq. 4 (Deng, 2003):

$$W_n = R_{cn}/R_c \quad (4)$$

Where W_n is strength retention coefficient, in which n is the days of sample immersing water; R_{cn} is the strength of the wet samples after immersion in water for n days; R_c is the strength of the dry samples cured for different days (e.g., 7 and 14 days).

Water Absorption

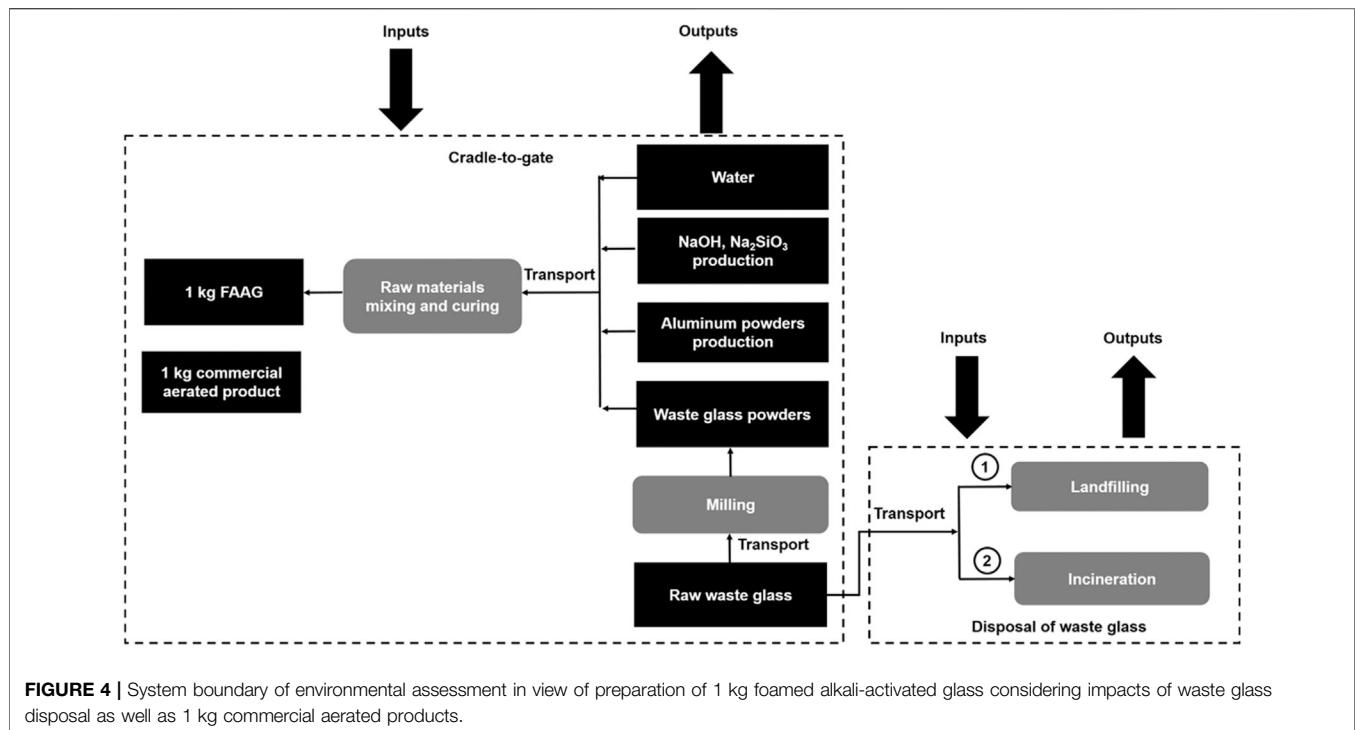
To determine the water absorption of the FAAG, three similar prisms were oven-dried at a temperature of 80°C for 24 h, and the dry weight was recorded as the initial weight. The samples were then immersed in water for 48 h, after which the saturated surface dry weight was recorded as the final weight. The calculation is shown below, according to ASTM (2012) in Eq. 5:

$$W\% = [(M_{\text{saturated}} - M_{\text{dry}})/M_{\text{dry}}] \times 100\% \quad (5)$$

Impact Resistance

The impact resistance of FAAG was determined using the Charpy testing method, in line with ASTM (2018). The Charpy testing method is based on the energy measurement expressed in energy (Joule) required to breaking the samples, shown in Figure 3. Since the maximum potential energy of the pendulum is known can be expressed as a function of the mass of the hammer and fall height,

**FIGURE 3** | (A) Setup of Charpy testing (CEAST Torino, United Kingdom) (B), (C) view of samples cut out to an appropriate size from different angles.



the energy absorbed can be calculated *via* the breakage of the samples (CEAST, 2008).

Thermal Conductivity

The thermal conductivity was measured with a thermal conductivity meter (Fox 200, TA Instruments, United States). The steady-state heat flux through the rectangular block sample was measured for a temperature gradient of 10°C between the upper and the lower face of the sample. Three identical 150 mm × 150 mm × 10 mm samples for each sample were measured for a more accurate result of thermal conductivity. Before measurement, the samples were left 24 h at 80°C and placed for 30 min in a dry chamber for cooling without moisture absorption.

X-ray Diffraction

To identify the newly formed phases in FAAG, a Bruker X-ray diffractometer (D8 Advance, Germany) was used with an automatic slit, monochromated Cu K α radiation ($\lambda = 1.5405 \text{ \AA}$), 15°–50° 2 θ range, with steps of 0.02°/2 θ and 0.5 sec/step. The raw material (i.e., waste glass) and the crushed FAAG samples after compression test with different amounts of the foaming agent were ground and sieved, and the powder was stored in ethanol for 3 days to stop hydration and dried prior to testing. Peaks were identified using the software DIFFRACT.SUITE (Bruker, Germany).

Environmental Assessment

SimaPro 8, as a software tool is used for life cycle assessment in this study. This section introduces the goal and system boundary, inventories, transportation, and impact assessment during the life cycle assessment (from cradle to gate) of the FAAG preparation as follows:

Goal and System Boundary

The goal of this part was to perform a life cycle assessment for the preparation of 1 kg FAAG, where the damage categories, CO₂ emissions and energy consumptions associated with its preparation were investigated, and the outcomes were compared with the equivalent amount of aerated commercial products (sand/gravel, quicklime, anhydrite, cement, and aluminium powder). Meanwhile, the impacts of waste glass disposal were avoided from the outcomes related to FAAG preparation during the assessment, and a similar idea was also widely reported in a number of environmental assessments (Zhao et al., 2009; He et al., 2019). **Figure 4** displays the system boundary of environmental assessment due to the preparation of 1 kg FAAG considering impacts of waste glass disposal and 1 kg commercial aerated product.

Inventories

Since the glass used in this study was regarded as pure municipal waste, any inputs and outputs associated with its production can be neglected. The inventories of the aerated commercial product were obtained from the database Ecoinvent (Version 2.0). To produce 1 kg of FAAG, the inputs and outputs related to the production of the rest of the raw materials, that is, NaOH, Na₂SiO₃, and aluminum powder, as well as electricity and transportation, were gained from the database Ecoinvent and ETH-ESU. To produce 1 kg of FAAG, 1 kg of waste glass, 119.6 g of water, 5.6 g of aluminum powder, 55.4 g of NaOH, and 166.4 g of Na₂SiO₃. The electricity is calculated to be 0.25 kWh, which is calculated through the power (i.e., 750 w) *time (i.e., 20 min) used in the milling of waste glass.

Transportation

Only the transportation of waste glass is considered, and the distance is assumed to be 2,000 km from Covilhã, Portugal to London, United Kingdom, and the travel distances of the rest raw materials, i.e., NaOH, NaSi₂O₃, and aluminum powder from a local factory or distributor to London, United Kingdom were assumed to be 650, 2,000, and 180 km, respectively. In view of the landfilling or incineration of waste glass, the travel distance of waste glass from Covilhã, Portugal to the nearest landfilling or incineration site was assumed to be 300 km. The means of transportation concerning all the materials were assumed to be by lorry.

Impact Assessment

The damage categories, including damage to health, ecosystem quality, and resources, were obtained by the Eco-indicator 99 approach. Furthermore, instead of a single score, a mixing triangle was used to tackle the weighting issues when making the decisions in terms of the selection of FAAG or the commercial aerated products, and the determination of points was obtained when they cross the boundaries of the triangle, and the indifference lines were drawn later (Hofstetter et al., 1999). The detained points calculated on the corresponding triangle sides were acquired *via* the calculation of Eqs 6–8.

$$WR = \{D_{HH}(A)/T_{HH} - D_{HH}(B)/T_{HH}\} / \{D_R(B)/T_R - D_R(A)/T_R + D_{HH}(A)/T_{HH} - D_{HH}(B)/T_{HH}\} \quad (6)$$

$$W_{HH} = \{D_R(B)/T_R - D_R(A)/T_R\} / \{D_R(B)/T_R - D_R(A)/T_R + D_{HH}(A)/T_{HH} - D_{HH}(B)/T_{HH}\} \quad (7)$$

$$W_{EQ} = \{D_R(B)/T_R - D_R(A)/T_R\} / \{D_R(B)/T_R - D_R(A)/T_R + D_{EQ}(A)/T_{EQ} - D_{EQ}(B)/T_{EQ}\} \quad (8)$$

Where $D_R(A)$, $D_{EQ}(A)$, $D_{HH}(A)$, $D_R(B)$, $D_{EQ}(B)$, and $D_{HH}(B)$ represent the damages of product A (i.e., FAAG) and B (i.e., the commercial aerated product) in terms of resources (R), ecosystem quality (EQ), and human health (HH), separately. The overall damages of each safeguard theme are referred to as T_R , T_{EQ} , and T_{HH} ; and W_R , W_{EQ} , and W_{HH} represent the weighting of the safeguard themes on the corresponding triangle side.

The CO₂ emissions of the preparation of 1 kg FAAG and 1 kg commercial aerated product were obtained *via* an Intergovernmental Panel on Climate Change 2007 approach (Pachauri and Reisinger, 2007) with a timeframe of 100 years. The energy consumptions associated with the sample preparations were calculated *via* the Cumulative Energy Demand method. The Cumulative Energy Demand method incorporates the sum of direct and indirect energy consumption (mega joule) throughout the entire life cycle, including the energy consumed during the production of raw materials and transportation (Bribián et al., 2011).

RESULTS AND DISCUSSION

Selection of Foamed Alkali-Activated Glass Formulation

The effects of aluminum powder content on the mechanical performance and the density of FAAG were investigated in

this section, facilitating the selection of FAAG formulation. **Figure 5** presents the pore structures of selected samples, indicating the excellent foaming performance of FAAG, which consists of a closed network of pores, regular in shape and distribution depending on the content of aluminium powder. **Figure 6** shows the density of FAAG reduced with the growth of aluminum powder content after 7 days of curing. The density of FAAG with 30% aluminum powder (i.e., 0.48 g/cm³) is 17.8% lower than the counterparts with 10% (i.e., 0.59 g/cm³). The latter is related to a higher amount of H₂ gas formed within this mixture, presenting a more porous structure, as seen in **Eq. 1**.

As expected, **Figure 6** also illustrates that FAAG with decreasing density led to inferior mechanical performance including compressive and flexural strength, and both compressive and flexural strength of FAAG with 30% aluminum powder is only 1/3 than the group with 10%. It is to be noted that when the amount of aluminum powder increased from 10 to 20%, there is nearly no decline in terms of the strength, and a possible explanation could be related to the instability of foams formed within the samples, which caused by the foam bubbles and a sudden reduction in vertical thickness of the system, as indicated by the large error bars in **Figure 6**, and Hajimohammadi et al. (2018) also reported that the foamed geopolymers *via* the chemical approach were not as controllable as the physical foamed ones. However, a growth of aluminum powder from 20 to 30% is accompanied by a great reduction in the strength and density due to the porous structure formed resulting from H₂ generation. Besides, the difference of irregularity of pore morphology and interconnections in samples containing 30% may also account for its great decline in the mechanical performance.

Albeit it presents the lowest density, FAAG with 30% aluminum powder was not considered due to its relatively low strength and a high amount of aluminum powder used, that is, a higher overall cost in terms of the sample preparation. The aluminum powder content in later FAAG preparation was fixed to 10% based on its similar mechanical performance with FAAG containing 20% of foaming agent, as well as cost-effectiveness *via* reducing the amount of foaming agent introduced. At the same time, the density of FAAG with 10% of foaming agent (i.e., 0.59 g/cm³) was not sacrificed compared with the group with 20% (i.e., 0.57 g/cm³), which is highly favored for the thermal insulation.

Performance of Selected Foamed Alkali-Activated Glass Samples

In this section, the results of mechanical performance, water resistance, water absorption, impact resistance, and thermal conductivity of the prepared FAAG were elaborated from *Mechanical Properties to Thermal Conductivity*.

Mechanical Properties

Mechanical performance is shown in **Figure 7**. To overcome the issue that the samples have a curved surface which was caused by the irregular foaming expansion of the system, the surface of each specimen was sanded down to achieve a straight and flat surface; allowing the force to be exerted evenly across the samples. Even

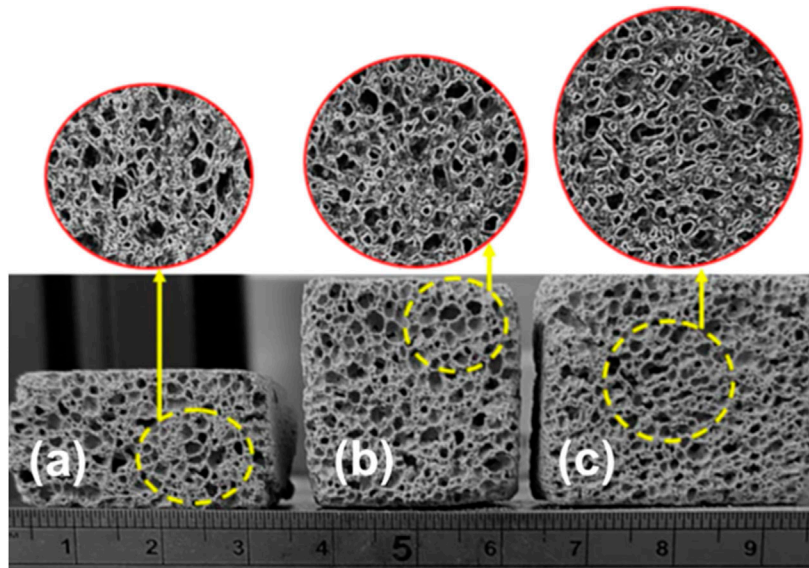


FIGURE 5 | Foamed alkali-activated glass containing (A) 10%; (B) 20% and (C) 30% aluminum powder via the use of the optical microscope, and the images were captured by a software (Scale label: x210).

though the error bars are still large in this figure, the figure still shows that the prepared FAAG reached a promising compressive and flexural strength of ≥ 5 MPa and ≥ 3 MPa, respectively after 28 days (Figure 7) due to the continuous hydration, showing high potential in not only insulation applications but also in lightweight secondary structural elements. Meanwhile, even considering the lower limit of the 28-days value in Figure 7, the compressive strength of the prepared FAAG can still be allocated to MU 5.0 grade (i.e., ≥ 5 MPa) from the Chinese standard (GB/T29062-2012, 2012).

Water Resistance and Absorption

The permeability of concrete is related with water absorption, which controls several concrete durability issues such as carbonation or chloride migration (De Schutter and Audenaert, 2004), whereas Brady et al. (2001) also reported that the permeability of foamed concrete has strongly relied on its porosity, and the size distribution as well as interconnectivity among pores. In practice, the water absorption of foamed products is of great significance since if this value is high when the foamed products are in storage or

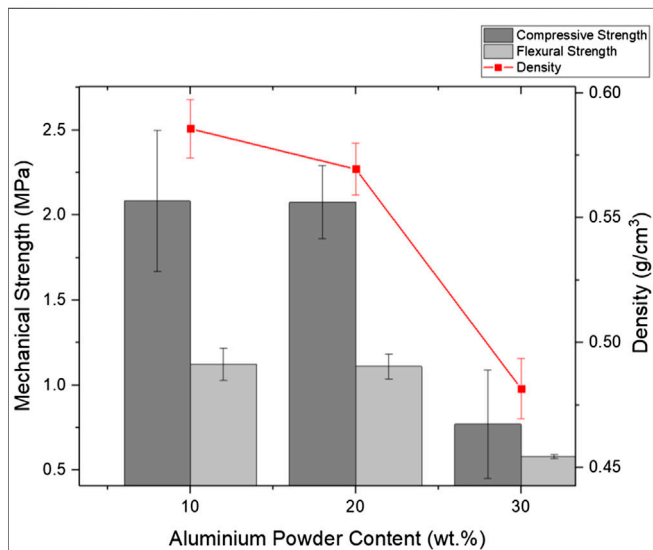


FIGURE 6 | Effect of aluminum powder content on the mechanical performance and density of foamed alkali-activated glass cured for 7 days.

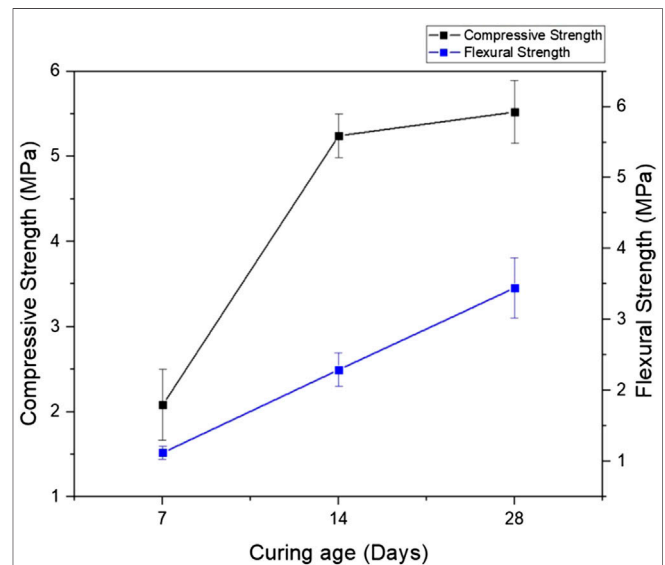
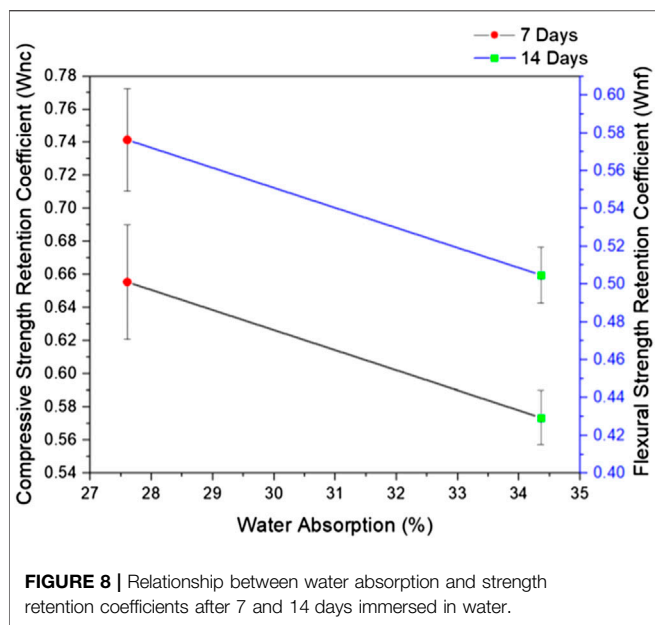


FIGURE 7 | Mechanical performance of the prepared foamed alkali-activated glass with different curing ages.



service, they would absorb moisture and become moldy in a humid environment, which would deteriorate their thermal insulation and mechanical performance. Therefore, the water absorption and resistance of FAAG were tested as an approach to assess its porosity (mainly capillary pores) and durability.

Figure 8 illustrates the relationship between the strength retention coefficients with the water absorption of prepared FAAG after 7 and 14 days of curing. The figure displays that the strength of FAAG decreases with the growth of water absorption. In the meantime, with the increase of immersion time, there is also a reduction in the strength retention coefficients of FAAG. Both compressive and flexural strength retention coefficients decreased to around 50% after 14 days of water exposure in contrast with non-submerged FAAG, and this could be ascribed to the fact that the additional water absorption further increases the formation of capillary pores in FAAG, leading to inferior mechanical performance during testing. Nambiar and Ramamurthy (2006, 2007) also reported that several factors control the water ingress into foamed concrete such as the pore distribution and tortuosity instead of the overall porosity, and the entrapped air failed to contribute to the transportation of water. Indeed, from *Selection of FAAG Formulation*, it seems that a large number of pores formed due to the entrapped H_2 in FAAG are disconnected, however, Wong et al. (2011) also demonstrated that there are interconnections between entrained voids facilitated by the capillary pores within the pore structure, thus offering a continuous path for the water ingress facilitated by the entrapped air voids within FAAG. Meanwhile, the air void-paste interface acts as an interfacial transition zone (ITZ) as well, which also promotes the movement of water, thus explaining its high water absorption of FAAG in this study (i.e., 7 days: 27.6%; 14 days: 34.4%).

The Chinese standard (GB/T29062-2012, 2012) reported that the 24-h water absorption of foamed products should be $\leq 25\%$ when their density grade is B11. Therefore, the water absorption

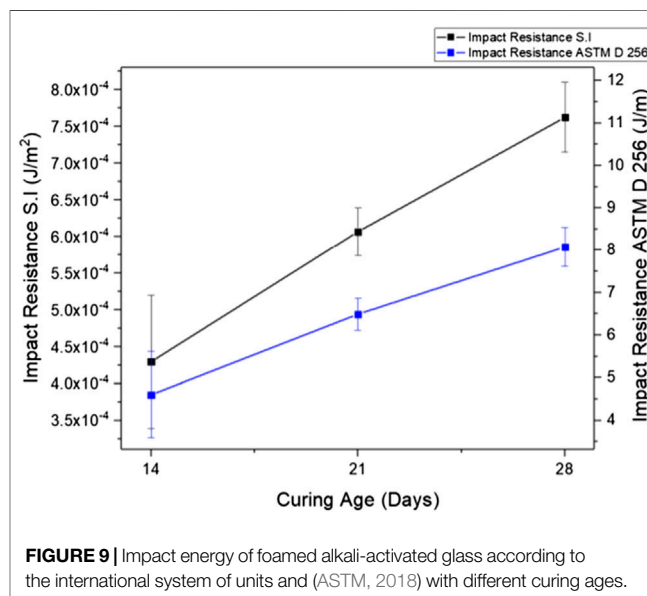
of the prepared FAAG is believed to satisfy the requirement considering the 7-days value, albeit the value is high.

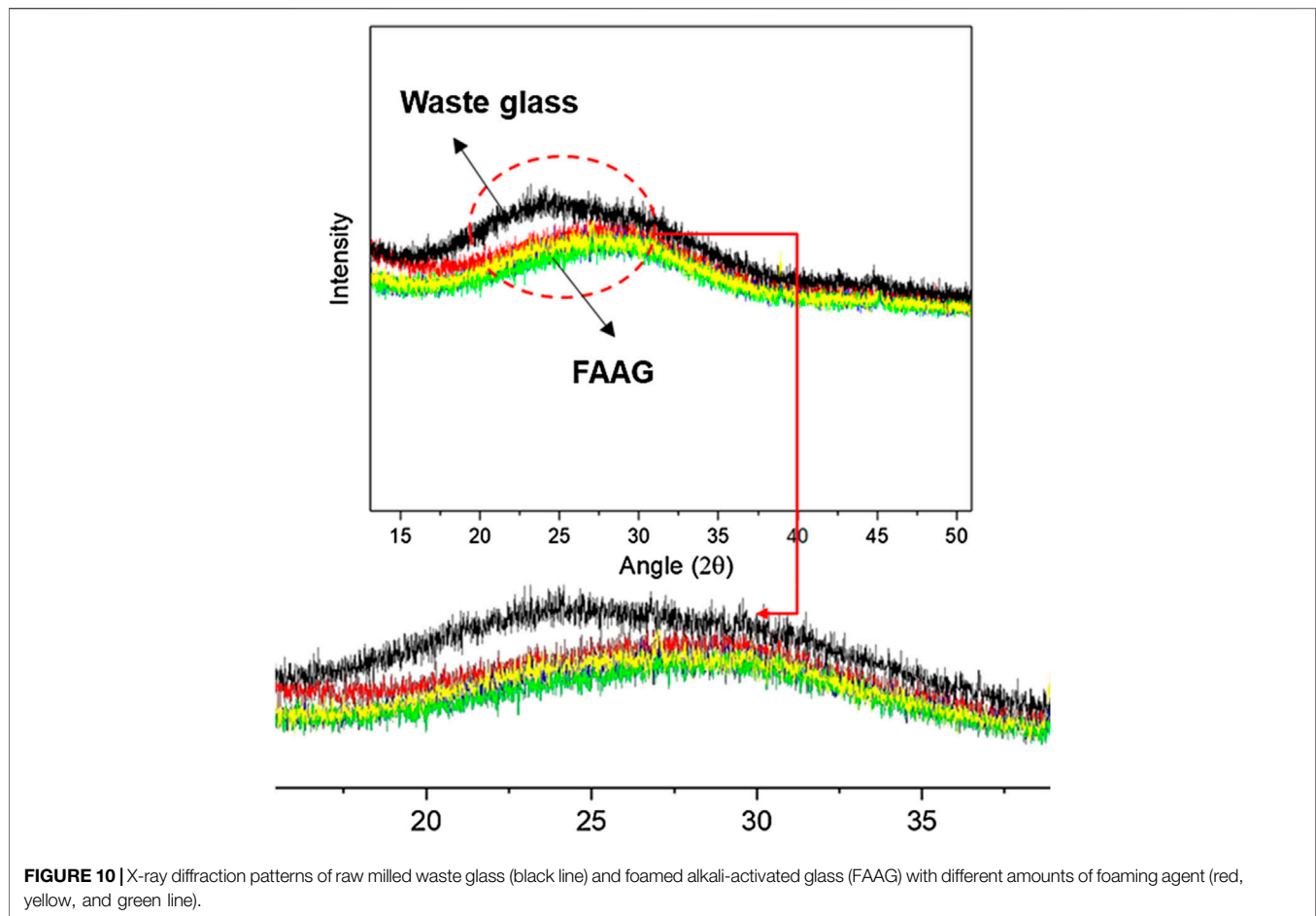
Impact Resistance

The Charpy testing method is used to investigate the impact resistance of FAAG. In this study, the impact energy of the FAAG was tested after 14, 21, and 28 days of curing age, as shown in **Figure 9**. The figure shows that the growth of curing age also led to an improvement of impact energy in the prepared FAAG. For instance, the impact energy of FAAG after 28 days of curing shows a 76.8% increment compared with the counterparts cured for 14 days. In geopolymers, alumina-silicate gels are the major phases that provide mechanical and bonding strength (Provis and Van Deventer, 2009). As expected, the impact resistance of FAAG is inferior in comparison with other ceramic-like and cementitious materials, which could be possibly related to the presence of ITZ between air voids and geopolymer paste, as discussed before. A large number of ITZ layers reduced the hardness of samples, leading to their lower energy absorption capacity and inferior impact resistance (Mohammadhosseini et al., 2017). The brittle nature of FAAG was also confirmed by the spalling of samples during the experiment.

Thermal Conductivity

A good formulation (Density: $\leq 1.15 \text{ g/cm}^3$; Compressive Strength: $\geq 5 \text{ MPa}$) of FAAG was selected based on the previous findings, and when the density grade of FAAG is B11, its thermal conductivity should be $\leq 0.32 \text{ W/(mK)}$ stipulated by the Chinese standard (GB/T29062-2012, 2012), thus only one thermal conductivity (i.e., the prepared FAAG) was measured in this section, and the rest two groups were not investigated. The thermal conductivity of FAAG obtained is $\sim 0.13 \text{ W/(mK)}$, which meets the Chinese specification.





Phase Transformation of Foamed Alkali-Activated Glass Samples

The phase transformation of FAAG is identified by XRD. **Figure 10** shows that the respective XRD patterns exhibited no reflections attributable to any identifiable crystalline phases, but only an amorphous hump is identified. The amorphous hump in the waste glass could be related to the presence of silica, but the hump was shifted toward (27° – 28°) 2-theta in FAAG, suggesting that some new gel phases formed during the activation of the FAAG, which could be assigned to the presence of aluminosilicate. It is reported that the geopolymerization needs individual alumina and silicate species, resulting the dissolution of silicon- and aluminum-containing sources materials at a high pH. Therefore, in view of this, aluminum powder is not only working as a foaming agent to produce a porous structure, but also involved in the process of geopolymerization within FAAG, facilitating the formation of amorphous aluminosilicate and contributing to the strength development of FAAG, which will be investigated in the future.

A Comparison Between the Foamed Alkali-Activated Glass and Other Existing Foamed Products in the Literature

Figure 11 shows a comparison between the FAAG and other existing foamed products in the literature. The figure clearly

indicates that the prepared FAAG in this study is capable of achieving either lower thermal conductivity or higher compressive strength than other existing foamed products. For instance, the FAAG developed in this study outperformed the cement-gypsum binders (Samson et al., 2017), the contaminated dredged river sediment foamed concrete (Yang et al., 2020) and the magnesium phosphate cement-based foamed concrete (Li et al., 2019) in terms of the strength (**Figure 11**). At the same time, the FAAG also presents slightly higher thermal conductivity but greater strength than some foamed products such as black dust-based autoclaved aerated concrete (Maneewan et al., 2019) and fly-ash based foamed geopolymer (Feng et al., 2015). The figure also shows that in terms of the compressive strength and thermal conductivity, the only foamed product that was comparable with the FAAG developed in this study is fly-ash based foamed geopolymer (Abdollahnejad et al., 2015).

Compared with the foamed glass, the production of FAAG eliminated the high sintering temperature used and the CO_2 emission during the foaming process. Meanwhile, the foamed glass selected from the literature presented much lower density [i.e., 0.15 g/cm^3 (Dragoescu et al., 2018); 0.12 g/cm^3 (König et al., 2019); 0.12 g/cm^3 (König et al., 2016); 0.44 g/cm^3 (Dragoescu et al., 2018)] than that of the FAAG (i.e., 0.59 g/cm^3), which led to their better thermal insulation performance [thermal conductivity: 0.024 – 0.051 W/(mK)], as well as inferior strength

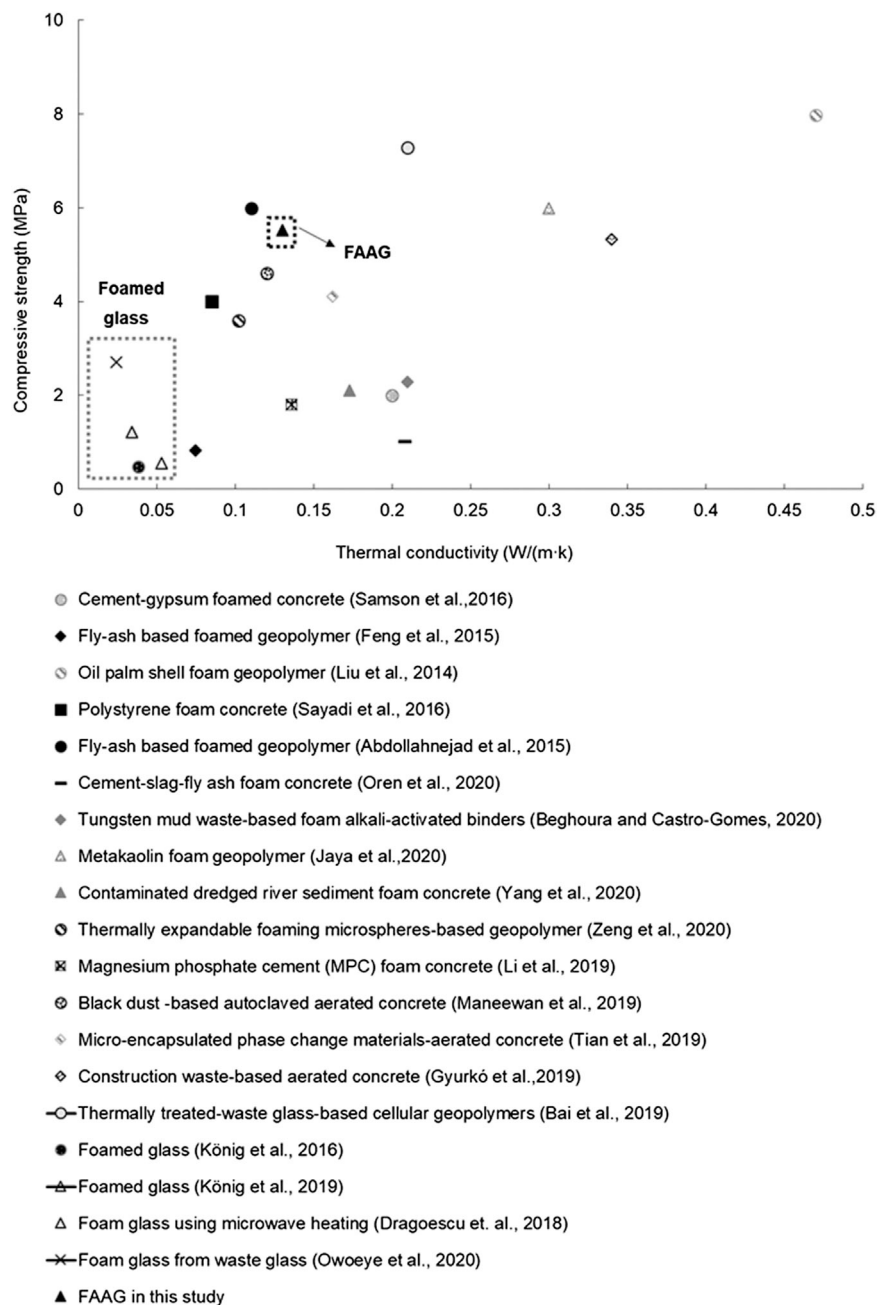


FIGURE 11 | Comparison between the prepared foamed alkali-activated glass (FAAG) and other foamed construction products.

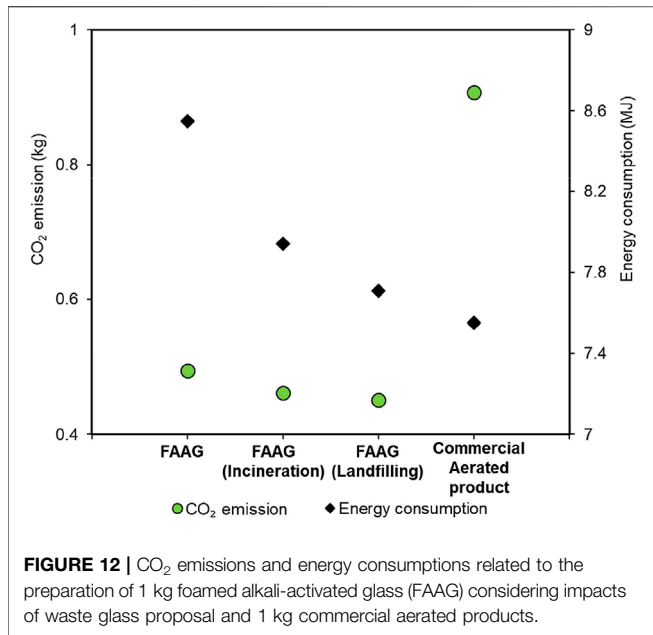
(i.e., 0.55–2.7 MPa) compared with the values of the FAAG developed in this study [i.e., 0.13 W/(mK) and 5.52 MPa], as shown in **Figure 11**. At the same time, the geopolymerization process within the FAAG also results in its better mechanical performance than that of the foamed glass.

Given the findings above, the simple comparison indicates that in this study, the synthesized FAAG in low-temperature revealed good mechanical performance, and the product developed is capable of competing with or outperform other existing

foamed products for thermal insulation, providing a feasible solution to the upcycling of waste glass in a large scale.

Environmental Assessment of the Selected Foamed Alkali-Activated Glass Preparation

Figure 12 presents the CO₂ emissions and energy consumptions related to the preparation of 1 kg FAAG and 1 kg commercial aerated products, where the environmental burdens associated with waste glass disposal were also considered. The figure clearly

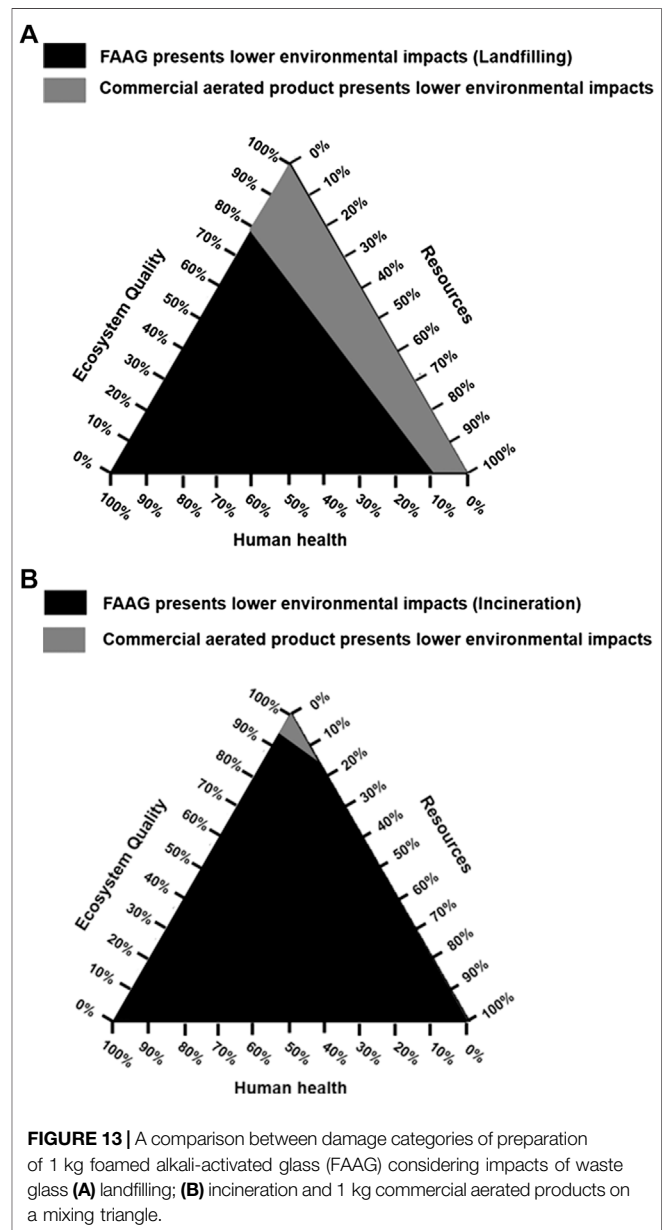


shows that the preparation of FAAG emits 45.5% less CO₂ than the commercial aerated products chosen from the database, which could be attributed to the involvement of PC in the manufacturing of commercial ones, as the production of PC leads to a large amount of greenhouse gas emission due to the decomposition of limestone in the kiln (Ruan and Unluer, 2016; Ruan and Unluer, 2017). In the meantime, since around 74.2% of total raw materials in FAAG preparation are a kind of pure waste, its neglected inventory also contributes to a reduced CO₂ emission in FAAG preparation. However, the preparation of the commercial aerated products had an advantage over FAAG in terms of the energy consumption (Figure 12), which could be attributed to the incorporation of alkali activator (i.e., NaOH and Na₂SiO₃) in FAAG preparation, albeit its content is low. It is known that the production of these alkali involves the technique of electrolysis, which is an energy-intensive process and leads to greater energy demand, and similar findings were also reported in our previous study (Kastiukas et al., 2020).

In addition, Figure 12 also presented that if the environmental impacts of waste glass disposal *via* landfilling or incineration were avoided in the outcomes of FAAG, its CO₂ emission and energy consumption could be further reduced. Besides, a larger decline rate in terms of the two indicators was achieved in FAAG containing waste glass that was supposed to be incinerated if not used in geopolymers preparation. A possible explanation could be related to the negligible emissions from waste glass landfill, as indicated by the database, and this process only consists of exchanges to process-specific burdens (i.e., energy and land use), and infrastructure, whereas with respect to the waste glass incineration, waste-specific air, and water emissions from incineration as well as auxiliary material consumption for flue gas cleaning were taken into account, which is also presented in the database. Further, the process of waste glass incineration

also consumed much electricity for the heating of materials. Hence, waste glass disposal through incineration led to a 2.1% larger quantity of CO₂ emission and 2.9% greater energy demand than through landfilling, accounting for the variations in Figure 12.

The mixing triangle was adopted to present a comparison between the damage categories of 1 kg FAAG and 1 kg commercial aerated products, in which the environmental impacts of waste glass disposal were also considered, as shown in Figure 13. The figure shows that when the impacts of waste glass landfilling or incineration were subtracted from the outcomes of FAAG preparation, the preparation of FAAG outperformed the commercial aerated products in reducing damages to human health, ecosystem quality, and resources, indicating its greater sustainability.



Therefore, given the above findings, FAAG can be regarded as a more sustainable construction product than the commercial one for thermal insulation.

CONCLUSIONS

Following the work from Kastiukas et al. (2020), indicated that in the United Kingdom, due to the shutdown of the electricity plants and the upgrade of equipment in the steel industry, there will be a shortage of fly ash and ground-granulated blast-furnace slag soon, which are widely used as precursors in the preparation of geopolymers previously. Therefore, the waste glass would provide an alternative precursor for the preparation of samples, especially the foamed products. Some specific conclusions were drawn as follows:

- (1) A low-temperature (i.e., 80°C) upcycling of waste glass is feasible to produce foamed glass, and a good formulation of FAAG was developed and prepared (i.e., the thermal conductivity of ~0.13 W/(mK; Density of ~0.59 g/cm³; Compressive strength of ~5.52 MPa). In addition to a foaming agent, aluminum powder is also working as a key component in the geopolymerization of waste glass, and the produced re-silicate within the samples led to the strength development of samples, indicating that milled waste glass with aluminum powder can be used to synthesize foamed product for thermal insulation.
- (2) The weak water and impact resistance of FAAG are related to their porous structure. Although the water absorption of FAAG is high (i.e., 7 days: 27.6%; 14 days: 34.4%), the value is still thought to be within the scope of the requirement stipulated by the Chinese standard.
- (3) In the area of thermal insulation, the FAAG developed in this study outperformed the commercial aerated products in reducing the CO₂ emissions and damages to human

REFERENCES

- Abdollahnejad, Z., Pacheco-Torgal, F., Félix, T., Tahri, W., and Barroso Aguiar, J. B. (2015). Mix design, properties and cost analysis of fly ash-based geopolymer foam. *Constr. Build. Mater.* 80, 18–30. doi:10.1016/j.conbuildmat.2015.01.063
- ASTM (2012). C642. *Standard test method for density, absorption, and voids in hardened concrete*. West Conshohocken, PA: ASTM International.
- ASTM (2017). C1585-17. *Standard test method for density of hydraulic cement*. West Conshohocken, PA: ASTM International.
- ASTM (2018). D256-10. *Standard test methods for determining the izod pendulum impact resistance of plastics*. West Conshohocken, PA: ASTM International
- Bai, C., Li, H., Bernardo, E., and Colombo, P. (2019). Waste-to-resource preparation of glass-containing foams from geopolymers. *Ceram. Int.* 45, 7196–7202. doi:10.1016/j.ceramint.2018.12.227
- Brady, K., Watts, G., and Jones, M. R. (2001). *Specification for foamed concrete*. United Kingdom: TRL Limited Crowthorne.
- Bribián, I. Z., Capilla, A. V., and Usón, A. A. (2011). Life cycle assessment of building materials: comparative analysis of energy and environmental impacts and evaluation of the eco-efficiency improvement potential. *Build. Environ.* 46, 1133–1140. doi:10.1016/j.buildenv.2010.12.002
- CEAST (2008). *Torino manual handbook*. Torino, Italy: Compagnia Europea Apparecchi Scientifici Torino (CEAST).Google Scholar

health, ecosystem quality and resources, indicating its greater sustainability than the commercial one.

Overall, this study endeavored to demonstrate mechanical performance, thermal conductivity, and environmental impacts. However, in practice, the durability of foamed products is of great significance, albeit their thermal conductivity and strength are also crucial, and the freeze-thaw, the wetting-drying cyclic test and the fire-resistance test will be the focus in our next-step. Moreover, the large variations of some values (e.g., compressive strength) obtained in this study are associated with the instability of the foaming process *via* a chemical approach, and this issue needs to be addressed in the future before the application of this foamed product.

DATA AVAILABILITY STATEMENT

The original contributions presented in the study are included in the article, further inquiries can be directed to the corresponding author.

AUTHOR CONTRIBUTIONS

SR: formal analysis; methodology. GK: resources; supervision; writing-original draft. SL: data curation; validation. XZ: Funding acquisition; writing-review and editing; project administration.

FUNDING

Finance support from the European Commission Horizon 2020 Research and Innovation Programme through the grant 723825 (i.e., the Green INSTRUCT project) is greatly acknowledged.

- Deng, D. (2003). The mechanism for soluble phosphates to improve the water resistance of magnesium oxychloride cement. *Cem. Concr. Res.* 33, 1311–1317. doi:10.1016/s0008-8846(03)00043-7
- De Schutter, G., and Audenaert, K. (2004). Evaluation of water absorption of concrete as a measure for resistance against carbonation and chloride migration. *Mater. Struct.* 37, 591. doi:10.1617/14045
- Dragoescu, M. F., Axinte, S. M., Paunescu, L., and Fiti, A. (2018). Foam glass with low apparent density and thermal conductivity produced by microwave heating. *Eur. J. Eng. Technol.* 6.
- EN196-1 (2016). *BS: methods of testing cement, determination of strength*. London, United Kingdom: BSI.
- European Commission (2020). *Communication from the commission to the European parliament the council the European economic and social committee and the committee of the regions a new circular economy action plan for a cleaner and more competitive Europe*. Brussels, Belgium: Office for Official Publications of the European Communities.
- Feng, J., Zhang, R., Gong, L., Li, Y., Cao, W., and Cheng, X. (2015). Development of porous fly ash-based geopolymer with low thermal conductivity. *Mater. Des.* 65, 529–533. doi:10.1016/j.matdes.2014.09.024
- GB/T29062-2012 (2012). *Autoclaved foam concrete bricks and block*. Beijing, China: National Standard of the People's Republic of China (NSPRC) [in Chinese].
- Gu, G., Xu, F., Ruan, S., Huang, X., Zhu, J., and Peng, C. (2020). Influence of precast foam on the pore structure and properties of fly ash-based geopolymer foams. *Constr. Build. Mater.* 256, 119410. doi:10.1016/j.conbuildmat.2020.119410

- Hajimohammadi, A., Ngo, T., and Mendis, P. (2018). Enhancing the strength of pre-made foams for foam concrete applications. *Cem. Concr. Compos.* 87, 164–171. doi:10.1016/j.cemconcomp.2017.12.014
- He, P., Hossain, M. U., Poon, C. S., and Tsang, D. C. W. (2019). Mechanical, durability and environmental aspects of magnesium oxychloride cement boards incorporating waste wood. *J. Clean. Prod.* 207, 391–399. doi:10.1016/j.jclepro.2018.10.015
- Hofstetter, P., Braunschweig, A., Mettler, T., Müller-Wenk, R., and Tietje, O. (1999). The mixing triangle: correlation and graphical decision support for LCA-based comparisons. *J. Ind. Ecol.* 3, 97–115. doi:10.1162/108819899569584
- Kastiukas, G., Ruan, S., Liang, S., and Zhou, X. (2020). Development of precast geopolymer concrete via oven and microwave radiation curing with an environmental assessment. *J. Clean. Prod.* 255, 120290. doi:10.1016/j.jclepro.2020.120290
- Kastiukas, G., and Zhou, X. (2017). Effects of waste glass on alkali-activated tungsten mining waste: composition and mechanical properties. *Mater. Struct.* 50, 194. doi:10.1617/s11527-017-1062-2
- König, J., Nemanič, V., Žumer, M., Petersen, R. R., Østergaard, M. B., and Yue, Y. et al. (2019). Evaluation of the contributions to the effective thermal conductivity of an open-porous-type foamed glass. *Constr. Build. Mater.* 214, 337–343. doi:10.1016/j.conbuildmat.2019.04.109
- König, J., Petersen, R. R., and Yue, Y. (2016). Influence of the glass particle size on the foaming process and physical characteristics of foam glasses. *J. Non-Crystal. Solids* 447, 190–197. doi:10.1016/j.jnoncrysol.2016.05.021
- Lebullenger, R., and Mear, F. O. (2019). “Glass recycling,” in *Springer handbook of glass*. New York, NY: Springer, 1355–1377.
- Li, T., Wang, Z., Zhou, T., He, Y., and Huang, F. (2019). Preparation and properties of magnesium phosphate cement foam concrete with H₂O₂ as foaming agent. *Constr. Build. Mater.* 205, 566–573. doi:10.1016/j.conbuildmat.2019.02.022
- Lu, J.-X., and Poon, C. S. (2018). Use of waste glass in alkali activated cement mortar. *Constr. Build. Mater.* 160, 399–407. doi:10.1016/j.conbuildmat.2017.11.080
- Lu, J.-X., Yan, X., He, P., and Poon, C. S. (2019). Sustainable design of pervious concrete using waste glass and recycled concrete aggregate. *J. Clean. Prod.* 234, 1102–1112. doi:10.1016/j.jclepro.2019.06.260
- Luhar, S., Cheng, T.-W., Nicolaidis, D., Luhar, I., Pnias, D., and Sakkas, K. (2019). Valorisation of glass waste for development of geopolymer composites - mechanical properties and rheological characteristics: a review. *Constr. Build. Mater.* 220, 547–564. doi:10.1016/j.conbuildmat.2019.06.041
- Ma, C., Long, G., Shi, Y., and Xie, Y. (2018). Preparation of cleaner one-part geopolymer by investigating different types of commercial sodium metasilicate in China. *J. Clean. Prod.* 201, 636–647. doi:10.1016/j.jclepro.2018.08.060
- Manewan, S., Janyoosuk, K., Hoy-yen, C., and Thongtha, A. (2019). Incorporating black dust into autoclaved aerated concrete wall for heat transfer reduction. *J. Met. Mater. Miner.* 29, 82–87. doi:10.14456
- Metro (XXXX). Glass: special glass products. Available at: <https://www.metroglass.com.nz/catalogue/072.aspx> (Accessed January 09, 2020).
- Mohammadhosseini, H., Abdul Awal, A. S. M., and Mohd Yatim, J. B. (2017). The impact resistance and mechanical properties of concrete reinforced with waste polypropylene carpet fibres. *Constr. Build. Mater.* 143, 147–157. doi:10.1016/j.conbuildmat.2017.03.109
- Nambiar, E. K. K., and Ramamurthy, K. (2006). Influence of filler type on the properties of foam concrete. *Cem. Concr. Compos.* 28, 475–480. doi:10.1016/j.cemconcomp.2005.12.001
- Nambiar, E. K. K., and Ramamurthy, K. (2007). Sorption characteristics of foam concrete. *Cem. Concr. Res.* 37, 1341–1347. doi:10.1016/j.cemconres.2007.05.010
- Østergaard, M. B., Petersen, R. R., König, J., Bockowski, M., and Yue, Y. (2019). Impact of gas composition on thermal conductivity of glass foams prepared via high-pressure sintering. *J. Non-Crystal. Solids* 1, 100014. doi:10.1016/j.nocx.2019.100014
- Pachauri, R. K., and Reisinger, A. (2007). *IPCC fourth assessment report*. Geneva, Switzerland: IPCC.
- Panda, B., Ruan, S., Unluer, C., and Tan, M. J. (2019). Improving the 3D printability of high volume fly ash mixtures via the use of nano attapulgite clay. *Compos. Part B Eng.* 165, 75–83. doi:10.1016/j.compositesb.2018.11.109
- Panda, B., Ruan, S., Unluer, C., and Tan, M. J. (2020). Investigation of the properties of alkali-activated slag mixes involving the use of nanoclay and nucleation seeds for 3D printing. *Compos. Part B Eng.* 186, 107826. doi:10.1016/j.compositesb.2020.107826
- Provis, J. L., and Van Deventer, J. S. J. (2009). *Geopolymers: structures, processing, properties and industrial applications*. New York, NY: Elsevier.
- Ruan, S., and Unluer, C. (2016). Comparative life cycle assessment of reactive MgO and Portland cement production. *J. Clean. Prod.* 137, 258–273. doi:10.1016/j.jclepro.2016.07.071
- Ruan, S., and Unluer, C. (2017). Influence of supplementary cementitious materials on the performance and environmental impacts of reactive magnesia cement concrete. *J. Clean. Prod.* 159, 62–73. doi:10.1016/j.jclepro.2017.05.044
- Samson, G., Phelipot-Mardelé, A., and Lanos, C. (2017). Thermal and mechanical properties of gypsum-cement foam concrete: effects of surfactant. *Eur. J. Environ. Civ. Eng.* 21, 1502–1521. doi:10.1080/19648189.2016.1177601
- Si, R., Dai, Q., Guo, S., and Wang, J. (2020). Mechanical property, nanopore structure and drying shrinkage of metakaolin-based geopolymer with waste glass powder. *J. Clean. Prod.* 242, 118502. doi:10.1016/j.jclepro.2019.118502
- Statista (2018). Key figures on glass recycling worldwide as of 2018. Available at: <https://www.statista.com/statistics/1055604/key-figures-glass-recycling-globally/> (Accessed January 22, 2020).
- Tchakouté, H. K., Rüscher, C. H., Kong, S., Kamseu, E., and Leonelli, C. (2016). Geopolymer binders from metakaolin using sodium waterglass from waste glass and rice husk ash as alternative activators: a comparative study. *Constr. Build. Mater.* 114, 276–289. doi:10.1016/j.conbuildmat.2016.03.184
- Torres-Carrasco, M., and Puertas, F. (2015). Waste glass in the geopolymer preparation. Mechanical and microstructural characterisation. *J. Clean. Prod.* 90, 397–408. doi:10.1016/j.jclepro.2014.11.074
- Vafaei, M., and Allahverdi, A. (2017). High strength geopolymer binder based on waste-glass powder. *Adv. Powder Technol.* 28, 215–222. doi:10.1016/j.apt.2016.09.034
- Wong, H. S., Pappas, A. M., Zimmerman, R. W., and Buenfeld, N. R. (2011). Effect of entrained air voids on the microstructure and mass transport properties of concrete. *Cem. Concr. Res.* 41, 1067–1077. doi:10.1016/j.cemconres.2011.06.013
- Xiao, R., Ma, Y., Jiang, X., Zhang, M., Zhang, Y., and Wang, Y. et al. (2020). Strength, microstructure, efflorescence behavior and environmental impacts of waste glass geopolymers cured at ambient temperature. *J. Clean. Prod.* 252, 119610. doi:10.1016/j.jclepro.2019.119610
- Xuan, D., Tang, P., and Poon, C. S. (2019). MSWIBA-based cellular alkali-activated concrete incorporating waste glass powder. *Cem. Concr. Compos.* 95, 128–136. doi:10.1016/j.cemconcomp.2018.10.018
- Yang, K., Zhong, M., Magee, B., Yang, C., Wang, C., and Zhu, X. et al. (2017). Investigation of effects of Portland cement fineness and alkali content on concrete plastic shrinkage cracking. *Constr. Build. Mater.* 144, 279–290. doi:10.1016/j.conbuildmat.2017.03.130
- Yang, X., Zhao, L., Haque, M. A., Chen, B., Ren, Z., and Cao, X. et al. (2020). Sustainable conversion of contaminated dredged river sediment into eco-friendly foamed concrete. *J. Clean. Prod.* 252, 119799. doi:10.1016/j.jclepro.2019.119799
- Zaman, A. U. (2010). Comparative study of municipal solid waste treatment technologies using life cycle assessment method. *Int. J. Environ. Sci. Technol.* 7, 225–234. doi:10.1007/bf03326132
- Zhao, Y., Wang, H. T., Lu, W. J., Damgaard, A., and Christensen, T. H. (2009). Life-cycle assessment of the municipal solid waste management system in Hangzhou, China (EASEWASTE). *Waste Manag. Res.* 27, 399–406. doi:10.1177/0734242X09103823
- Zhu, X., Zhang, Z., Yang, K., Magee, B., Wang, Y., and Yu, L. et al. (2018). Characterisation of pore structure development of alkali-activated slag cement during early hydration using electrical responses. *Cem. Concr Compos* 89, 139–149. doi:10.1016/j.cemconcomp.2018.02.016

Conflict of Interest: The authors declare that the research was conducted in the absence of any commercial or financial relationships that could be construed as a potential conflict of interest.

Copyright © 2020 Ruan, Kastiukas, Liang and Zhou. This is an open-access article distributed under the terms of the Creative Commons Attribution License (CC BY). The use, distribution or reproduction in other forums is permitted, provided the original author(s) and the copyright owner(s) are credited and that the original publication in this journal is cited, in accordance with accepted academic practice. No use, distribution or reproduction is permitted which does not comply with these terms.